

Crystal Structure Study of (*E*)-3-(4-Nitrobenzyloxyimino)-hexahydroazepin-2-one Using Synchrotron Radiation

D. TranQui,^{a*} S. Raymond,^b J. Pecaut^a and Å. Kvick^c

^aLaboratoire de Cristallographie-CNRS Associé à l'Université Joseph Fourier, 25 Avenue des Martyrs, BP 166, F-38042 Grenoble CEDEX, France, ^bCentre de Recherche sur les Macromolécules Végétales and Université Joseph Fourier, BP 53, F-38041 Grenoble CEDEX, France, and ^cEuropean Synchrotron Radiation Facility, BP 220, F-38043 Grenoble CEDEX, France. E-mail: tranqui@labs.polycnrs-gre.fr

(Received 5 July 1996; accepted 8 January 1997)

NOHA, 3-(4-nitrobenzyloxyimino)hexahydroazepin-2-one, is a potent anticonvulsive agent. It occurs in two stereoisomers, the *Z* and *E* forms. (*E*)-NOHA is about 1.5 times more active than (*Z*)-NOHA. While accurate structural data are available for (*Z*)-NOHA, those for the *E* form have remained, until recently, highly speculative due to the lack of single crystals of suitable size for X-ray analysis and to the instability of the *E* isomer under radiation exposure. For structure–activity correlation purposes, efforts have been made to solve the crystal structure of the *E* isomer. Data collection from tiny needle crystals has been performed using synchrotron radiation. An initial molecular-packing model of this compound was obtained by energy-based and X-ray data modelling and successfully refined by molecular-dynamics methods: space group $P2_1/c$, $a = 6.225(5)$, $b = 17.885(5)$, $c = 12.157(5)$ Å, $\beta = 92.35(5)^\circ$, R factor = 3.5% for 343 reflections. In this contribution the crystal and molecular structure of (*E*)-NOHA is reported and the role of the hydrogen bond acting as the driving force in the intermolecular assembly in the (*E*)-NOHA crystal is highlighted.

Keywords: crystal structure; nitrobenzyl oximinoether; microdiffraction; molecular dynamics; computer modelling.

1. Introduction

In the search for new molecules with relaxant activity, one family of compounds, the oximinocaprolactam derivatives, were identified as potential anticonvulsive candidates. Preliminary pharmacological tests *in vitro* on the 3-(4-nitrobenzyloxyimino)hexahydroazepin-2-one member or NOHA indicate that this compound displays an anticonvulsive activity almost comparable with that of well known compounds such as theophylline or cromakalim (Elfrom, 1995).

Cross-reference studies of NOHA suggest that its activity strongly depends on the nature and the position of different functional groups of the molecule. Thus, changing the position of NO₂ on the phenyl group in NOHA or substitution of the caprolactam, a seven-membered heterocycle (C₆NOH), by a benzene ring results in a dramatic drop in its activity. In addition, thin-layer chromatography and NMR studies indicate that NOHA actually has two stereoisomers, the *Z* and *E* forms. Subsequent tests have shown that the *E* isomer is 1.5 times more potent than the *Z* form.

Structural data of the oximinocaprolactam derivatives, in particular those of the two most active stereoisomers of NOHA, are therefore needed to understand better their structure–activity correlation. The crystal structure of the (*Z*)-NOHA isomer has been recently characterized by X-rays (TranQui, Elfrom, Pera & Leclerc, 1996); that

of (*E*)-NOHA, because of the lack of single crystals with suitable size for structure analysis by a conventional X-ray source, has been estimated by molecular modelling and NMR data and therefore remains highly speculative.

Efforts have been made to model the structure of the *E* isomer using incomplete and low-resolution X-ray data collected at ESRF.

2. Experimental

Owing to their very small size, no experiments on crystals of (*E*)-NOHA could be performed using our in-house X-ray equipment. Several transparent needle-shape crystals with average sizes oscillating around $150 \times 16 \times 18$ μm were glued onto a thin-walled Lindemann capillary tube. The experiments were performed on beamline 2 (ID11) of the ESRF (Kvick & Wulf, 1992). Monochromatic radiation with a wavelength of 0.6199 Å was used. Diffraction spots were recorded by the oscillation crystal technique on image-plate surfaces positioned at 303 mm from the crystal and scanned with a Molecular Dynamics Phosphor Imager 400E device. Comparison of the first and the last image-plate pictures indicated that the crystal was severely damaged by X-ray exposure. To overcome this last-minute trouble and to prevent possible difficulties in indexing the oscillation pictures in the present case, *i.e.* small unit cell, the

Table 1Crystal data, data collection and structure refinement of (*E*)-NOHA.

Identification code	(<i>E</i>)-NOHA
Empirical formula	C ₁₃ H ₁₅ N ₃ O ₄
Formula weight	277.28
Temperature	293 (2) K
Wavelength	0.6199 (5) Å
Crystal system	Monoclinic
Space group	<i>P</i> 2 ₁ / <i>c</i>
Unit-cell dimensions	<i>a</i> = 6.225 (5) Å <i>b</i> = 17.885 (5) Å <i>c</i> = 12.157 (5) Å β = 92.35 (5)°
Volume	1352.4 (13) Å ³
<i>Z</i>	4
Density (calculated)	1.362 Mg m ⁻³
Absorption coefficient	0.103 mm ⁻¹
Crystal size	0.14 × 0.02 × 0.01 mm
θ range for data collection	1.77–14.1°
Index ranges	−3 ≤ <i>h</i> ≤ 4 −9 ≤ <i>k</i> ≤ 10 −5 ≤ <i>l</i> ≤ 6
Reflections collected	739
Overall <i>R</i> _{int}	0.056
Independent reflections	343 (<i>R</i> _{int} = 0.1022)
Refinement method	Full-matrix least squares on <i>F</i> ²
Data/restraints/parameters	343/106/184
Goodness-of-fit on <i>F</i> ²	0.621
Final <i>R</i> indices [<i>I</i> > 2σ(<i>I</i>)]	<i>R</i> ₁ = 0.0352, <i>wR</i> ₂ = 0.0966
<i>R</i> indices (all data, 368 reflections)	<i>R</i> ₁ = 0.0492, <i>wR</i> ₂ = 0.1984
Largest diffraction peak and hole	0.109 and −0.091 e Å ⁻³

experiments were conducted in two steps. (*a*) The first four images of each crystal were recorded in a large $\Delta\omega_a$ oscillation angle of 60° with an overlap angle of 20°; the exposure time of each picture was $\tau_a = 29$ s. (*b*) Using the same crystal with the same angular settings a second image set was taken with $\Delta\omega_b = 18^\circ$ and $\tau_a = 12$ s. Steps (*a*) and (*b*) were repeated for three different crystals. Two data sets recorded in steps (*b*), belonging to two different samples, were successfully indexed and their unit cells were identified. Fortunately they were identical, within the limit of experimental errors. Systematic extinction rules of observed reflections indicated that the space group was *P*2₁/*c* (Table 1). Based on the above unit-cell parameters, and after repeated manual interventions using *DENZO* (Otwinowski, 1993; Gewirth, 1993), *FIT2D* (Hammersley, 1993; Hammersley, Svensson & Thompson, 1993) and our own software, most of the diffraction spots recorded in step (*a*) were indexed and processed. Finally, a total of 739 intensities observed above the 2σ(*F*²) level and averaged to only 343 unique reflections with *F*² > 2σ(*F*²) in the low-resolution range (no reflections with 2θ > 14° were observed) were obtained after scaling, merging and Lorentz–polarization correction. The determination of the crystal structure of such a compound (containing 20 non-H atoms), under unfavourable experimental conditions, small size and instability of the sample, using only 343 low-resolution reflections was a difficult challenge. However, the determination is worthwhile because, as stated above, of its pharmacological interest and also because the results of this work show that the quality of a synchrotron X-ray

Table 2Atomic coordinates (× 10⁴) and equivalent isotropic displacement parameters (Å² × 10³) for (*E*)-NOHA.

	<i>x</i>	<i>y</i>	<i>z</i>	<i>U</i> _{eq}
O1	8842 (13)	4888 (3)	3171 (5)	87 (3)
O2	5825 (13)	4646 (4)	2292 (7)	94 (3)
O3	2064 (10)	2903 (5)	6960 (4)	61 (3)
O4	−1314 (8)	1938 (3)	7786 (6)	77 (3)
N1	7036 (22)	4630 (5)	3098 (12)	60 (4)
N2	2695 (15)	2228 (6)	6511 (6)	55 (3)
N3	−2620 (20)	1974 (3)	6059 (8)	53 (3)
C1	6259 (22)	4270 (5)	4113 (13)	45 (4)
C2	7549 (17)	4254 (5)	5050 (12)	57 (4)
C3	6787 (20)	3954 (5)	5998 (10)	64 (4)
C4	4753 (20)	3653 (5)	6037 (11)	46 (4)
C5	3477 (15)	3670 (4)	5071 (12)	47 (3)
C6	4201 (18)	3974 (5)	4087 (10)	48 (4)
C7	3897 (18)	3373 (5)	7082 (9)	68 (4)
C8	1243 (22)	1751 (7)	6393 (7)	44 (4)
C9	−935 (21)	1918 (4)	6793 (13)	47 (4)
C10	−2281 (12)	1964 (5)	4863 (9)	73 (3)
C11	−1525 (13)	1216 (5)	4426 (6)	84 (3)
C12	839 (13)	1062 (4)	4640 (7)	71 (3)
C13	1538 (12)	1031 (5)	5839 (7)	60 (3)

*U*_{eq} is defined as one third of the trace of the orthogonalized *U*_{ij} tensor.

beam combined with computer modelling techniques and a molecular-dynamics refinement strategy constitute powerful synergetic factors to overcome ‘difficult crystal structure’ problems. Attempts to solve the structure of the *E* form by direct methods turned out to be unsuccessful. This is due to the fact that direct methods work poorly with high incompleteness and low-resolution data.

Hence, the crystal structure of the *E* isomer was directly modelled assuming (*a*) that the molecular conformation of the *E* isomer was close to that of the *Z* isomer (thus, the molecular geometry of the *E* isomer was kept rigid), and (*b*) that the periodicity of the packing scheme of *E* molecules should be consistent with the unit-cell parameters and symmetry observed by X-rays. The *Packer* program (*Cerius* 1.5; Molecular Simulations Inc., 1994) was initially used to conduct the modelling. It generated 11 low-energy packing models. The non-bonded contacts of these models looked reasonable but none of them corresponded to the observed X-ray data. Furthermore, inspection of difference Fourier maps of the refined models confirmed that the crystal structure solution of the *E* isomer was indeed not included in these models. One of the reasons for this failure was that the model assumption, (*a*), proved to be incorrect.

In other attempts based on a heuristic approach devised by TranQui *et al.* (1995), the molecule was partitioned into several rigid building blocks except for the oximinoether moiety. To limit the number of parameters, only torsion angles involving the C7(*sp*³) atom of the oximinoether function were considered. Only three torsion angles, C8—N2—O3—C7, N2—O3—C7—C4 and O3—C7—C4—C3, were allowed to distort almost freely by associating low force constant values (*A*₁, *A*₂ and *A*₃) to the above torsional shifts. A fourth angle, C9—C8—N2—O3, was kept rigid because a rotation around C8—N2 would be hindered on the one hand by the large size of the C₆NO

Table 3
Selected bond distances (Å) and angles (°) for *(E)*-NOHA.

O1—N1	1.216 (9)	C2—C3	1.374 (8)
O2—N1	1.211 (9)	C3—C4	1.378 (8)
O3—N2	1.387 (7)	C4—C5	1.391 (8)
O3—C7	1.421 (8)	C4—C7	1.485 (11)
O4—C9	1.241 (12)	C5—C6	1.405 (8)
N1—C1	1.490 (13)	C8—C13	1.468 (9)
N2—C8	1.247 (9)	C8—C9	1.489 (10)
N3—C9	1.352 (10)	C10—C11	1.521 (8)
N3—C10	1.478 (9)	C11—C12	1.510 (8)
C1—C2	1.368 (8)	C12—C13	1.505 (9)
C1—C6	1.385 (8)	N3...N2 ⁱ	3.024 (12)
N2—O3—C7	108.5 (8)	C4—C5—C6	122.4 (12)
O1—N1—O2	126 (2)	C1—C6—C5	117.2 (11)
O1—N1—C1	115.8 (13)	O3—C7—C4	115.1 (9)
O2—N1—C1	117.9 (14)	N2—C8—C13	123.3 (14)
C8—N2—O3	115.1 (13)	N2—C8—C9	119.4 (12)
C9—N3—C10	120.6 (14)	C13—C8—C9	117.2 (11)
C2—C1—C6	121.5 (14)	O4—C9—N3	118 (2)
C2—C1—N1	120.0 (14)	O4—C9—C8	122.4 (11)
C6—C1—N1	119 (2)	N3—C9—C8	120 (2)
C1—C2—C3	119.7 (13)	N3—C10—C11	114.3 (8)
C2—C3—C4	122.1 (13)	C12—C11—C10	114.4 (7)
C3—C4—C5	117.1 (14)	C11—C12—C13	114.5 (7)
C3—C4—C7	121.5 (12)	C8—C13—C12	112.0 (7)
C5—C4—C7	121.2 (13)	N3—H...N2 ⁱ	166.9 (11)
	Isomer <i>E</i>	Isomer <i>Z</i>	
C8—N2—O3—C7	177.7 (7)	−179.0 (4)	
N2—O3—C7—C4	69.8 (8)	−178.2 (3)	
O3—C7—C4—C3	−163.7 (7)	150.8 (4)	

Symmetry code: (i) $x - 1, y, z$.

group and on the other hand by the double-bond character of the C8—N2 bond.

Furthermore, the force-constant assignment may be modified in the course of the energy-optimization search. The target function to be minimized, as widely used in the refinement of macromolecules, consisted of an empirical energy term and the crystallographic-type residual term. The *X-PLOR* program (Brünger, 1992) was used to conduct the search and refinements. Local minima were eliminated by a simulated annealing strategy.

After inspection of the best results of several series of simulated annealing refinements using different sets of A1, A2 and A3 used in the construction of the target function, it turned out that low A2 (*i.e.* high flexibility around torsion angle O3—C7—C4—C3) tended to give the best results. A new series of simulated annealing refinements with A3 = 20, A1 = 80 and A2 = 35 led to an *R* factor of 27%. At this stage, the model, considered to be close enough to the crystal structure solution, was successfully refined using conventional difference Fourier and, because of the low ratio of observed reflections to model parameters, extensive restrained least-squares refinements. The calculations were performed at the last stage with the *SHELXL93* program (Sheldrick, 1993) which led to an *R* factor of 3.5% (the weighted wR_2 value was 9.7%) for 343 reflections with $F^2 > 2\sigma(F^2)$. All H-atom positions which were geometrically calculated were excluded in the refinements. A low weighted *R* factor and low residual electron-density peak (or hole) heights (Table 1) suggest that the data obtained under the experimental conditions described above are of

good quality. However, because of the small number of observed reflections the e.s.d. values of bond lengths and bond angles remain large. Thus, in the following, we focus our comparative discussion on the *E* and *Z* isomers only in terms of conformational aspects.

3. Results and discussion

Crystal-data, data-collection and structure-refinement results are summarized in Table 1.* Atomic coordinates and equivalent isotropic thermal factors are given in Table 2 and selected bond lengths and bond angles are given in Table 3. For comparison purposes, the *ORTEP* plot of the *E* isomer is represented along with that of the *Z* isomer in Figs. 1(a) and 1(b). As shown in Fig. 1(a), the molecule

* A list of structure factors has been deposited with the IUCR (Reference R10003). Copies may be obtained through The Managing Editor, International Union of Crystallography, 5 Abbey Square, Chester CH1 2HU, England.

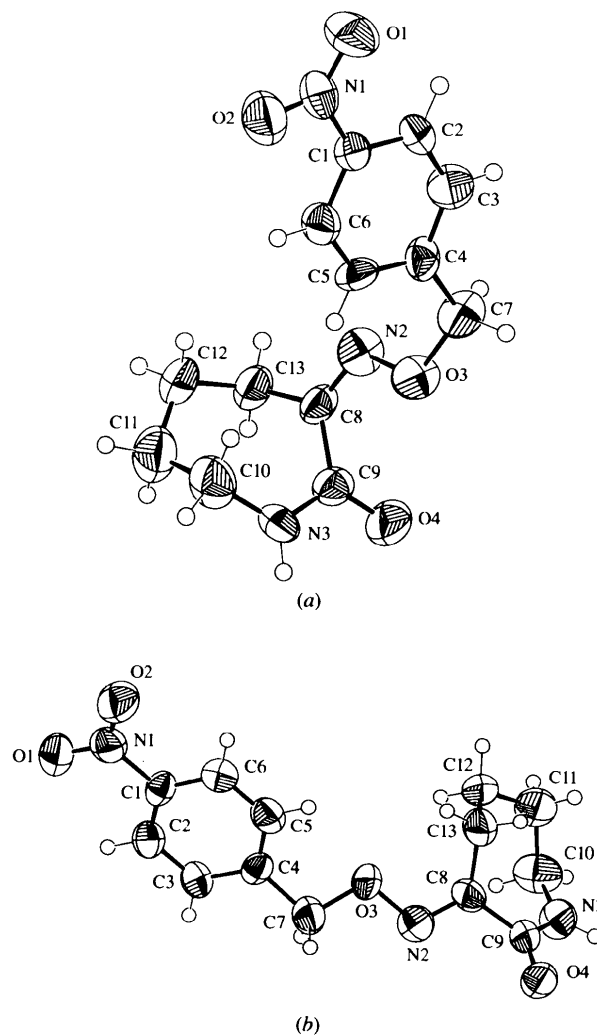


Figure 1
Representations of (a) the *E* isomer and (b) the *Z* isomer of 3-(4-nitrobenzyloxyimino)hexahydroazepin-2-one (*XTAL GX*; Hall & du Boulay, 1995).

of the *E* isomer consists of a non-planar seven-membered heterocycle, C₆NO, and a planar nitrobenzene ring linked together through the oximinoether function. Although the bond-angle values are less accurate than those of the *Z* form, they are fairly similar to those observed in the *Z* isomer, indicating that the geometry of the two terminal groups in both isomers is not distorted by the molecular-packing force. The differences in the torsion angles in the *Z* and *E* isomers clearly indicate the flexibility of the oximinoether segment. Using the Newman projections around the C7—C4 and O3—C7 bonds in both cases, it appears that the isomers can be interconverted by rotation of appropriate torsion angles in the oximinoether group. Thus, a rotation of 14° around C7—C4 followed by another

one of 112° around the O3—C7 bond axis would almost superpose the C₆NO of the *Z* isomer on that of the *E* isomer. As a result of this double rotation, the molecule of the *E* isomer becomes less elongated than that of the *Z* isomer: the largest dimension of the molecular envelope of the *E* isomer is only 9.7 Å compared with 11.5 Å for the *Z* isomer. In addition, unlike with the *Z* isomer, the N2 lone pair in the *E* isomer is directed out on the molecular surface in such a way as it allows N2 to accept a hydrogen bond.

Thus, the crystal packing of the *E* isomer is mostly stabilized on the one hand, as expected, by benzene–benzene ring-stacking interactions with a ring–ring distance of 3.5 Å, and on the other hand by N3—H3···N2 hydrogen bonds. As illustrated in Figs. 3(a) and 3(b), the same N3 atom of the hexahydroazepine group acts as donor in both isomers, while N2 and O4 are the acceptors in the *E* and *Z* species, respectively. This results in different hydrogen-bond patterns in the two isomers: in the *Z* isomer the two N3—H···O4 bonds form a cyclic dimer of (*E*)-NOHA sitting across the centre of inversion corresponding to graph set R₂²(8) (Etter, MacDonald & Bernstein, 1990). The hydrogen-bond pattern in the *E* isomer is of linear type: molecules of the *E* isomer are linked to each other through the N3—H3···N2 bond forming an ‘infinite’ chain parallel to the shortest *a* axis of the unit cell, *i.e.* the most developed needle axis of the crystal.

Unlike the cyclic dimer, the chain pattern in the *E* isomer is somewhat unexpected because it generally requires severe constraints on the size and shape of the molecule. In the present case it is achieved by double rotations of torsion angles, as described above.

We are grateful to Drs J. P. Lauriat and E. Elkaim for their assistance in preliminary experiments at LURE, and special thanks to Dr H. Chanzy for his help in performing the data collection at ESRF and for stimulating discussions.

References

- Brünger, A. T. (1992). *X-PLOR Manual*. Version 2.1. Yale University, New Haven, USA.
- Elfrom, H. (1995). Thesis. Université Joseph Fourier, Grenoble France.
- Etter, M. C., MacDonald, J. C. & Bernstein, J. (1990). *Acta Cryst.* **B46**, 256–262.
- Gewirth, D. (1993). *DENZO Manual*. Department of Molecular Biophysics and Biochemistry, Yale University and the Howard Hughes Medical Institute, New Haven, CT 06511, USA.
- Hall, S. R. & du Boulay, D. (1995). *XTALGX User's Guide*. University of Western Australia, Australia.
- Hammersley, A. H. (1993). *FIT2D Reference Manual*. ESRF Internal Report EXP/AH/93-02. ESRF, Grenoble, France.
- Hammersley, A. H., Svensson, S. O. & Thompson, A. (1993). *Nucl. Instrum. Methods Phys. Res. A*, **346**, 312–321.
- Kvick, Å. & Wulf, M. (1992). *Rev. Sci. Instrum.* **63**, 1073–1076.
- Molecular Simulations Inc. (1994). *Cerius 1.5*. Molecular Simulations Inc., New England Executive Park, Burlington, MA 01803, USA.
- Otwinowski, Z. (1993). *Proceedings of the CCP4 Study Weekend: Data Collection and Processing*, edited by L. Sawyer, N. Isaacs & S. Bailey, pp. 52–62. SERC Daresbury Laboratory, Warrington, UK.

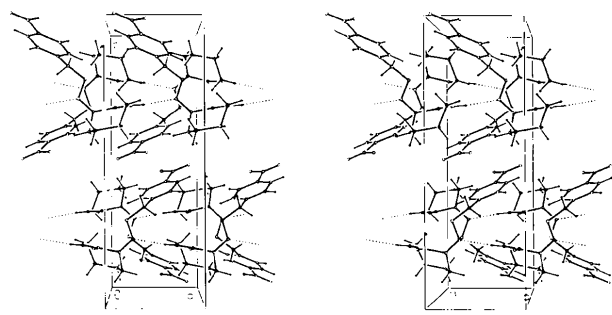


Figure 2
Packing diagram for (*E*)-3-(4-nitrobenzyloxyimino)hexahydroazepin-2-one.

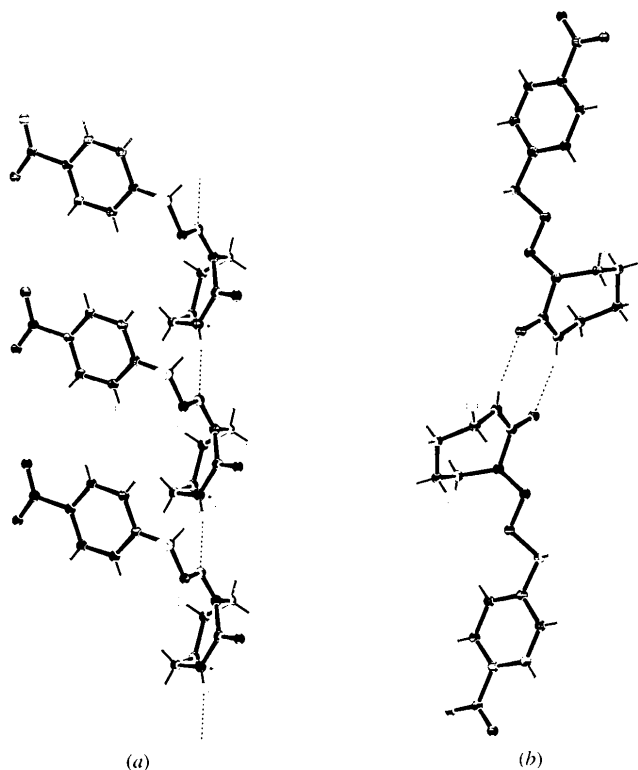


Figure 3
Hydrogen-bond pattern in 3-(4-nitrobenzyloxyimino)hexahydroazepin-2-one: (a) the *E* isomer, and (b) the *Z* isomer (PLUTON92; Spek, 1992).

Sheldrick, G. M. (1993). *SHELXL93. Program for Crystal Structure Refinement*. University of Göttingen, Germany.

Spek, A. L. (1992). *PLUTON92. An Interactive Graphics Program for Molecules*. University of Utrecht, The Netherlands.

TranQui, D., Elfrom, H., Pera, H. & Leclerc, G. (1996). *Acta Cryst. C52*, 2880–2882.

TranQui, D., Hermoso, J. A., Averbuch, M. T., Tamagnan, G., Leclerc, G. & Cussac, M. (1995). *Acta. Cryst. B51*, 77–80.